Anal. Chem. **2004,** *76,* 3646−3654

Scanning Electrochemical Microscopy: Theory and Characterization of Electrodes of Finite Conical Geometry

Cynthia G. Zoski,*,† Biao Liu,‡ and Allen J. Bard‡

Department of Chemistry, Georgia State University, Atlanta, Georgia 30303, and Department of Chemistry and Biochemistry, University of Texas at Austin, Austin, Texas 78712

Finite conical electrodes, which are of particular interest as probes for imaging of surfaces using scanning electrochemical microscopy (SECM), in kinetic studies and in probing thin films were investigated. Theoretical SECM tip current-distance feedback (approach) curves for a finite conical electrode were calculated by numerical (finite element) analysis and compared to an earlier approximate model. The SECM curves obtained depended on the ratio of the base radius of the cone to the height of the cone and on the thickness of the insulating sheath. A new approach to fabricating conical tips of Pt in glass is described. These were used to obtain approach curves over both electrically conducting and insulating substrates. Comparison of experimental and simulated SECM approach curves provided a sensitive method of evaluating the size and shape of finite conical electrodes.

Finite conical-shaped electrodes are of special interest in connection with the imaging of surfaces,[1−4] in kinetic studies,[5,6] and in probing thin films.[7] The most common fabrication procedure is by etching of carbon fibers or metal microwires to a sharp point followed by coating with an insulating material except at the apex of the tip.[1−5,8−13] Insulating materials have included glass,[8,9] Apiezon wax,[14] and electrophoretic paint.[5,12,15−18] Characterization of insulated etched electrodes has been carried out by a combination of scanning electron microscopy (SEM), steady-state voltammetry (SSV), and scanning electrochemical microscopy (SECM).[3,4,11,19] From SEM micrographs, the shape of etched electrodes has most often been described as conical because they are sharp at the apex and broad at the base where the metal and insulator meet.[4,8−11] Steady-state voltammetric experiments produce retraceable, sigmoidal current versus potential ($i-E$) curves, which are characteristic of ultramicroelectrodes (UMEs).[8−13] The steady-state limiting current based on the assumption of a hemispherical or inlaid disk geometry has been used most often to obtain an estimate of the radius of an etched electrode[3−6,8,9,12] because the theories for these geometries are well-established. The radius of etched electrodes has also been determined using a recently reported theory for steady-state limiting currents at finite conical electrodes.[20] SECM experiments using etched electrodes as the tip electrode have shown that the geometry is closer to conical than to either a disk or a hemisphere[4,7,19] based on a comparison of experimental data to an approximate model.[19]

Electrode characterization with SECM is based on approach curve measurements of a UME tip current (i_T) as a function of the tip−substrate separation (d)[21,22] over either a conducting or an insulating substrate. If an oxidizing species is reduced at the tip ($O + ne \rightarrow R$) and a conductive substrate is at a sufficiently positive potential, the tip-generated R is oxidized back to O at the substrate, and positive feedback is said to occur as the UME tip approaches the substrate. At insulating substrates, no oxidation of R occurs, and the approach curve is characterized as showing negative feedback where i_T decreases as d decreases. Experimental approach curves are then compared to theoretical ones. A range of UME tip geometries including inlaid disks,[11,21]

* Corresponding author e-mail: checgz@panther.gsu.edu.
† Georgia State University.
‡ University of Texas at Austin.

(1) Liu, H.-Y.; Fan, F.-R. F.; Lin, C. W.; Bard, A. J. *J. Am. Chem. Soc.* **1986**, *108*, 3838.
(2) Gewirth, A. A.; Craston, D. H.; Bard, A. J. *J. Electroanal. Chem.* **1989**, *261*, 477.
(3) Treutler, T. H.; Wittstock, G. *Electrochim. Acta* **2003**, *48*, 2923.
(4) Macpherson, J. V.; Unwin, P. R. *Anal. Chem.* **2000**, *72*, 276.
(5) Conyers, J. L., Jr.; White, H. S. *Anal. Chem.* **2000**, *75*, 3962.
(6) Watkins, J. J.; Chen, J.; White, H. S. *Anal. Chem.* **2003**, *72*, 4441.
(7) Mirkin, M. V.; Fan, F.-R. F.; Bard, A. J. *Science* **1992**, *257*, 364.
(8) Penner, R. M.; Heben, M. J.; Lewis, N. S. *Anal. Chem.* **1989**, *61*, 1630.
(9) Penner, R. M.; Heben, M. J.; Longin, T. L.; Lewis, N. S. *Science* **1991**, *250*, 1118.
(10) Kawagoe, K. T.; Jankowski, J. A.; Wightman, R. M. *Anal. Chem.* **1991**, *63*, 1589.
(11) Shao, Y.; Mirkin, M. V.; Fish, G.; Kokotov, S.; Palanker, D.; Lewis, A. *Anal. Chem.* **1997**, *69*, 1627.
(12) Slevin, C. J.; Gray, N. J.; Macpherson, J. V.; Webb, M. A.; Unwin, P. R. *Electrochem. Commun.* **1999**, *1*, 282.
(13) Maus, R.; Wightman, R. M. *Anal. Chem.* **2001**, *73*, 3993.
(14) Nagahara, L. A.; Thundat, T.; Lindsay, S. M. *Rev. Sci. Instrum.* **1989**, *60*, 3128.
(15) Schulte, A.; Chow, R. H. *Anal. Chem.* **1996**, *68*, 3054.
(16) Bach, C. E.; Nichols, R. J.; Meyer, H.; Shulte, A.; Besenhard, J. O. *Surf. Coat. Technol.* **1994**, *67*, 139.
(17) Bach, C. E.; Nichols, R. J.; Beckmann, W.; Meyer, H.; Shulte, A.; Besenhard, J. O.; Jannakoudakis, P. D. *J. Electrochem. Soc.* **1993**, *140*, 1281−1284.
(18) Mao, B. W.; Ye, J. H.; Zhuo, X. D.; Mu, J. Q.; Fen, Z. D.; Eian, Z. W. *Ultramicroscopy* **1992**, *42−44*, 464.
(19) Mirkin, M. V.; Fan, F.-R. F.; Bard, A. J. *J. Electroanal. Chem.* **1992**, *328*, 47.
(20) Zoski, C. G.; Mirkin, M. V. *Anal. Chem.* **2002**, *74*, 1986.
(21) *Scanning Electrochemical Microscopy*; Bard, A. J., Mirkin, M. V., Eds.; Marcel Dekker: New York, 2001.
(22) Bard, A. J.; Fan, F.-R. F.; Mirkin, M. V. In *Electroanalytical Chemistry*; Bard, A. J., Ed.; Marcel Dekker: New York, 1994; Vol. 18, pp 243−373.

10.1021/ac049938r CCC: $27.50
Published on Web 05/07/2004

hemispheres,[23,24] spheres,[25] rings,[26] ring-disks,[27] and etched electrodes[4,19] have been characterized in this way. Thus, a unique advantage of SECM is its sensitivity to the geometrical parameters of a UME tip, including the insulating sheath. This is in contrast to using the steady-state limiting current from a cyclic voltammogram. It has been demonstrated theoretically[28] and more recently experimentally[6] that the steady-state behavior of a UME is not a sensitive way of assessing UME shape, although it can be used to estimate the overall area of a UME.

The first theoretical study of the SECM feedback response was reported for disk-shaped tips using a finite element method (FEM).[29] A table of SECM tip current as a function of tip−substrate distance was reported for the relative thicknesses of the insulating sheath (RG = r_g/a, where r_g is the radius of the insulating sheath and a is the radius of the disk) of 10, 100, and 1000. An approximate analytical expression was reported that fit the simulated data for positive feedback. This analytical expression was later improved and fit specifically to the RG = 10 simulated data of ref 29 for positive feedback, and an analytical approximation for an insulating substrate was also reported for the RG = 10 data of that paper.[19] More recent SECM simulations of disk-shaped tips over insulators and conductors have included diffusion from behind the glass sheath of the UME tip as a function of RG, and analytical approximations with constants specific for each RG have been reported.[30,31] SECM responses with tip geometries including spheres,[32] hemispheres,[23,24,32,33] rings,[26] ring-disks,[27] and conical[33] tips have also been performed using numerical simulations based on the boundary element method (BEM), the alternating direction implicit method (ADIFDM), and FEM. Comparison with experimental approach curves have been reported only for hemispherical,[23,24] ring,[26] and ring-disk[27] UME tips.

The earliest model of a SECM-like arrangement in which nondisk electrodes were treated as thin-layer cell arrangements included twin hemispherical cells, hemisphere/plane cells, twin conical cells, and conical/plane cells.[34] Approximate expressions for the steady-state current were obtained for each thin-cell arrangement by modeling each electrode as a series of contiguous, thin circular strips with each approximating a parallel-plate electrode of equivalent area. The fluxes of the electroactive species to and from these strips were assumed to be parallel to the axis of symmetry passing through both electrodes. Thus, the approximation implied that each strip of one electrode communicated electrochemically with only the corresponding strip on the other electrode. The current generated by the thin-layer cell was then approximated by summing the individual currents generated by the series of parallel-plate electrodes. This model was found to accurately represent SECM steady-state currents when a UME tip is very close to a substrate because thin-layer approximations are in effect. However, the model was found to be invalid outside of the thin-layer region where the UME tip steady-state current ($i_{T,\infty}$) becomes important. Thus, the model was later refined so that a SECM approach curve over a planar substrate could be approximated when the UME tip was shaped as either a cone or a spherical segment. The diffusional flux to each strip on the UME tip was calculated using the approximate equation for a disk-shaped UME tip of RG = 10 over a conductive substrate:[19]

$$i_T(L)/i_{T,\infty} = 0.68 + 0.78377/L + 0.3315\exp(-1.0672/L) \quad (1)$$

where $L = d/a$ is the normalized distance or that for a disk-shaped UME tip over an insulating substrate is[19]

$$i_T/i_{T,\infty} = 1/[0.292 + 1.5151/L + 0.6553\exp(-2.4035/L)] \quad (2)$$

where

$$i_{T,\infty} = 4nFDc^b a \quad (3)$$

for an inlaid disk electrode[35] of RG = ∞ and at an infinite distance from the substrate. The normalized current to the nonplanar UME tip was then found by integrating the current over the entire UME tip surface. This approximate theory has been used in the characterization of etched electrodes[4,19] and hemispherical electrodes.[23]

Despite several reports of SECM with finite conical electrodes, there has been no rigorous description of the theory of SECM response with a finite conical-shaped tip with respect to geometry and the RG of the surrounding insulation. We report here the study of the steady-state SECM tip current as a function of tip−substrate distance at a finite conical UME and compare the results to the approximate theory reported earlier.[19] The numerical solution of the partial differential equations was carried out with PDEase 2D,[21,36] a commercial program employing finite element analysis. The comparison of theoretical SECM approach curves with experimental ones provided information about tip geometry including the ratio of the height of the finite cone to its base radius ($h/a = H$) and the relative thickness of the insulating sheath (RG).

EXPERIMENTAL SECTION

Materials. Ferrocenemethanol (Aldrich, Milwaukee, WI), KCl (EM Industries, Inc.), $CaCl_2$ (Matheson Cleman & Bell, Norwood, OH), and HCl (EM Science, Gibbstown, NJ) were reagent grade and used without further purification. All solutions were prepared with 18 MΩ·cm deionized water (Milli-Q, Millipore Corp.).

Electrochemical and SECM Experiments. Electrochemical experiments were performed in a Teflon cell (3-mL capacity) with a Pt wire (Goodfellow Metals) counter and a saturated Hg/Hg_2SO_4, K_2SO_4 (Radiometer, Copenhagen, Denmark) reference electrode. A CH Instruments (Austin, TX) model 900 SECM was used to perform all steady-state voltammetry and SECM measure-

(23) Selzer, Y.; Mandler, D. *Anal. Chem.* **2000**, *72*, 2383.
(24) Mauzeroll, J.; Hueske, E. A.; Bard, A. J. *Anal. Chem.* **2003**, *75*, 3880.
(25) Demaille, C.; Brust, M. B.; Tsionsky, M.; Bard, A. J. *Anal. Chem.* **1997**, *69*, 2323.
(26) Lee, Y.; Amemiya, S.; Bard, A. J. *Anal. Chem.* **2001**, *73*, 2261.
(27) Liljeroth, P.; Johans, C.; Slevin, C. J.; Quinn, B. M.; Kontturi, K. *Anal. Chem.* **2002**, *74*, 1972.
(28) Myland, J. C.; Oldham, K. B. *J. Electroanal. Chem.* **1990**, *288*, 1.
(29) Kwak, J.; Bard, A. J. *Anal. Chem.* **1989**, *61*, 1221.
(30) Shao, Y.; Mirkin, M. V. *J. Phys. Chem.* **1998**, *102*, 9915.
(31) Amphlett, J. L.; Denuault, G. *Anal. Chem.* **1998**, *102*, 9946.
(32) Fulian, Q.; Fisher, A. C.; Denuault, G. *J. Phys. Chem.* **1999**, *103*, 4393.
(33) Fulian, Q.; Fisher, A. C.; Denuault, G. *J. Phys. Chem.* **1999**, *103*, 4387.
(34) Davis, J. M.; Fan, F.-R. F.; Bard, A. J. *J. Electroanal. Chem.* **1987**, *238*, 9.
(35) Saito, Y. *Rev. Polarogr.* **1968**, 15, 177.
(36) *PDEase2D*, Version 3.0; Macsyma, Inc.: Arlington, MA, 1982−1998.

ments. A 2 mm diameter Pt disk (CH Instruments) served as the substrate. Approach curves were obtained either over the Pt conductor (positive feedback) or over the insulation surrounding the Pt disk (negative feedback). The substrate was mounted on an adjustable platform so that compensation for any substrate tilt could be made. All experiments were performed at room temperature.

Finite Conical Tip Fabrication. The conical Pt microelectrodes were constructed from 25 μm diameter Pt wire (Goodfellow, Cambridge, UK). A 2-cm-long Pt microwire was connected to a Cu wire with silver epoxy (Epotek, H20E, Epoxy Technology, Inc., Billerica, MA). The Pt wire was then electrochemically etched in a solution containing saturated $CaCl_2$ (60 vol %), H_2O (36%), and concentrated HCl (4%) (see ref 21, pp 78−80). About 1 mm of the wire was immersed in the solution. An ac voltage of ~10 V rms was applied between the Pt wire and a large-area carbon plate electrode using a Variac transformer. As the etching proceeded at the air/solution interface, bubbles formed at the Pt/solution interface. The power was switched off immediately upon cessation of bubbling as the top part of the electrode in air lost contact with the solution. The electrode shape at this point was not perfectly conical and had a longer sharp protrusion from the tip. This was "trimmed" by very rapidly immersing the tip under power back into the etching solution for very short (<1 s) periods several times. After "trimming", the wire was thoroughly rinsed with deionized water (Milli-Q, Millipore Corp).

The etched wire was dipped for ~3 s in a 3:1 HCl:HNO_3 solution to clean the Pt surface, and it was thoroughly rinsed with deionized water and then dried in an oven. With the help of microscopy (Olympus, BH-2), the etched Pt wire was inserted into one end of a pulled glass capillary prepared as described below with an inner diameter of ~20 μm such that the sharp end of the Pt tip was flush with the capillary opening, which was then melted around the Pt wire by using a gas/oxygen flame. Careful control of the flame temperature and heating time is critical to obtaining a well-sealed tip. Thus, the Pt tip/capillary assembly was held in the cone part of the flame near the nozzle outlet for approximately 2 s. The melted glass retracts from the tip on cooling; it is not necessary to invert the tip for this to happen. The success rate for making these tips was about 50%.

The glass capillary was prepared by pulling a borosilicate glass tube (o.d. = 1.0 mm, i.d. = 0.58 mm) with a micropipet puller (model P-2000, Sutter Instrument Co., Novato, CA). A one-line program was used in the pulling with the parameters heat = 300, filament = 4, velocity = 35, delay = 200, and pull = 0.

THEORY OF FINITE CONICAL ELECTRODES IN SECM

The geometry of a finite conical electrode is described by three parameters: the base radius (a) of the cone, the height (h), and the radius of the insulating sheath (r_g), as shown in Figure 1 or, alternatively, by a, r_g, and the aspect ratio $H = h/a$. Here we describe the steady-state tip current as a function of the distance between a tip and a substrate at a finite conical electrode studied using a numerical solution of relevant equations.

We consider the simple electron-transfer reaction:

$$\mathrm{O\ (soln)} + n\mathrm{e} \rightarrow \mathrm{R\ (soln)} \qquad (4)$$

at a finite conical electrode surface surrounded by insulation

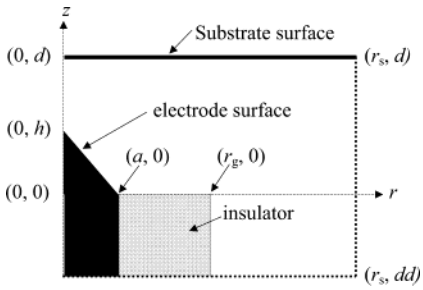

Figure 1. Diagram of a finite conical electrode in cylindrical coordinates and geometry of the simulation space.

(Figure 1) under conditions in which species O reaches and species R leaves the electrode solely by diffusion. The concentration of species O is given as $c(r,z,t)$, and the diffusion equation in cylindrical coordinates is described as

$$\frac{\partial c}{\partial t} = D\left(\frac{\partial^2 c}{\partial r^2} + \frac{1}{r}\frac{\partial c}{\partial r} + \frac{\partial^2 c}{\partial z^2}\right) \qquad (5)$$

where r and z are the coordinates in directions parallel and normal to the electrode base plane, respectively; t represents time; c is the concentration of O; and D is the diffusion coefficient of species O. For convenience, normalized dimensionless variables are introduced as follows:

$$R = r/a \qquad (6a)$$

$$Z = z/a \qquad (6b)$$

$$C = c(r,z,t)/c^{\mathrm{b}} \qquad (6c)$$

$$H = h/a \qquad (6d)$$

$$L = d/a \qquad (6e)$$

$$\mathrm{LL} = \mathrm{dd}/a \qquad (6f)$$

$$\mathrm{RG} = r_g/a \qquad (6g)$$

$$\mathrm{RS} = r_s/a \qquad (6h)$$

where a is the base radius of the cone, c^{b} is the bulk concentration of O, d is the tip−substrate separation, dd is the distance to the simulation limit behind the electrode surface, r_g is the insulator radius, and r_s is the simulation space limit.

Recently, it was demonstrate that finite conical electrodes reach a steady-state.[20] Since we are only interested in the steady-state system, the following diffusion equation was used for the calculations:

$$\frac{\partial^2 C}{\partial R^2} + \frac{1}{R}\frac{\partial C}{\partial R} + \frac{\partial^2 C}{\partial Z^2} = 0 \quad \text{at steady state} \qquad (7)$$

The digital simulation for a finite conical SECM tip was performed by calculating the diffusion-controlled steady-state current (i_T) at different tip−substrate distances (d) over substrates. The mixed boundary conditions are given by the following at steady state:

For a conductive substrate:

$$\partial C(0,Z)/\partial R = 0 \quad H \le Z < L \quad \text{axis of symmetry} \quad (8)$$

$$\partial C(\mathrm{RG},Z)/\partial R = 0 \quad \mathrm{LL} \le Z < 0 \quad \text{insulation below base plane} \quad (9)$$

$$\partial C(R,0)/\partial Z \quad 1 \le R < \mathrm{RG} \quad \text{insulation region} \quad (10)$$

$$C(\mathrm{RS},Z) = 1 \quad \mathrm{LL} < Z < L \quad \text{simulation limit} \quad (11)$$

$$C(R,\mathrm{LL}) = 1 \quad \mathrm{RG} < R < \mathrm{RS} \quad \text{simulation limit} \quad (12)$$

$$C(R,H(1-R)) = 0 \quad 0 \le R < 1 \quad \text{cone surface} \quad (13)$$

$$C(R,L) = 1 \quad 0 \le R < \mathrm{RS} \quad \text{substrate surface} \quad (14a)$$

For an insulating substrate:

$$\partial C(R,L)/\partial Z = 0 \quad 0 \le R < \mathrm{RS} \quad \text{substrate surface} \quad (14b)$$

The tip current to the entire surface of a finite conical electrode can be obtained as a function of tip−substrate distance by integrating the flux over the cone side (L_c):

$$i_T(L) = 2\pi nFDca \int_0^{L_c} R(\partial C/\partial N)\, dX \quad (15)$$

where $\partial C/\partial N = [(\partial C/\partial Z)\cos\alpha + (\partial C/\partial R)\sin\alpha]_{Z=H(1-R)}$ is the normal derivative of concentration at the finite cone surface, α is the angle at the base of the cone, $L_c = 1/\cos\alpha$, and X is the integration variable.

Finally, the tip current was normalized to give $I_T = i_T(L)/i_{T,\infty}$, where $i_{T,\infty}$ is the tip current when the electrode is located far from the substrate. The numerical solution of the diffusion equation was carried out with the program PDEase2D (Macsyma Inc., Arlington, MA), a commercial program that employs finite element analysis.[21,36] The details of using this program for a conical geometry under steady-state conditions have been described.[20] Application to other UME geometries in a SECM configuration include disks,[30,37] rings,[26] and hemispheres.[24]

RESULTS AND DISCUSSION

Steady-State Diffusion-Limited Current. The limiting currents of finite conical electrodes are needed in order to characterize the SECM response because tip currents are usually normalized by the $d \rightarrow \infty$ limiting currents. An investigation of the steady-state diffusion-limiting currents at finite conical electrodes using numerical (finite element) analysis was recently reported.[20] Tabulated values as well as approximate analytical expressions were developed to account for the geometrical dependencies of the aspect ratio H of the finite cone and the thickness RG of the insulating sheath. Aspect ratios of 0, 0.5, 1, 2, and 3 were considered, with RG ranging from 100 (infinite planar sheath) to 1.2. Additional aspect ratios considered in this work included H = 0.1 and 0.3. The normalized diffusion-limited steady-state currents for the aspect ratios considered in this work are tabulated in Table 1 for RG values of 10, 5, 2, and 1.2.

(37) Mirkin, M. V. In *Scanning Electrochemical Microscopy*; Bard, A. J., Mirkin, M. V., Eds.; Marcel Dekker: New York, 2001.

Table 1. Normalized Diffusion-Limited Steady-State Currents ($i_{T,\infty}/nFDc^b a$) at Finite Conical UMEs

RG	$H = 0$	$H = 0.1$	$H = 0.3$	$H = 0.5$	$H = 1.0$	$H = 2.0$	$H = 3.0$
10	4.072	4.165	4.372	4.608	5.320	6.924	8.556
5	4.156	4.257	4.469	4.712	5.460	7.152	8.892
2	4.440	4.546	4.794	5.080	5.932	7.872	9.824
1.2	4.952	5.078	5.362	5.700	6.660	8.768	10.780

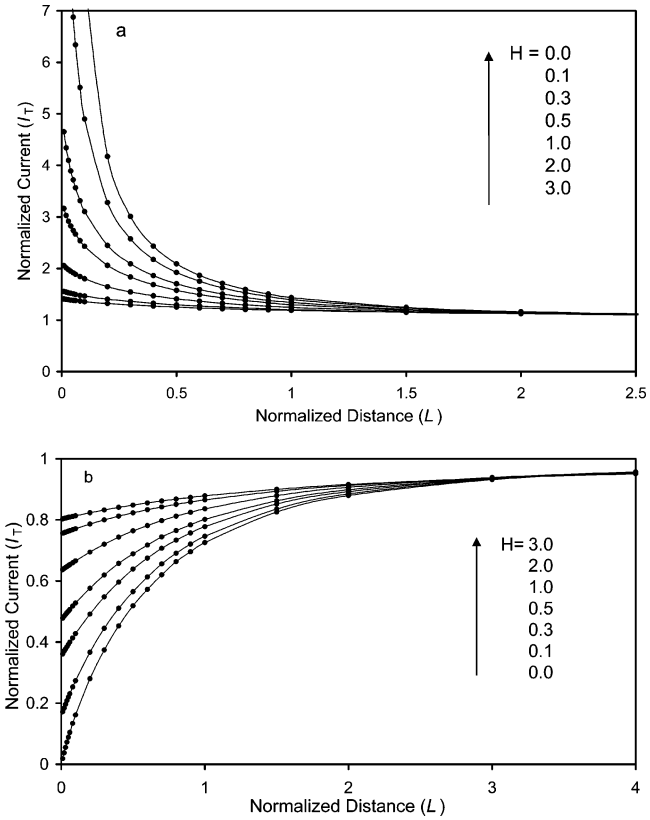

Figure 2. Theoretical SECM feedback responses of finite conical microelectrodes at (a) conductive and (b) insulating substrates with various H values while RG = 2.

SECM Approach Curves for Finite Conical Microelectrodes. The normalized tip current was calculated to obtain SECM approach curves for conical electrodes at various normalized distances (L) between the electrode and substrate. To characterize the SECM response of conical electrodes depending on the base radius and the height, simulated SECM curves were obtained with a varying aspect ratio H while keeping RG fixed. Figure 2 shows theoretical SECM feedback responses of conical electrodes when RG = 2. Compared to disk electrodes ($H = 0$), conical electrodes must approach closer to the substrate to reach a similar value of feedback current for a conductive substrate. For example, conical electrodes with $H = 0.5$ need to be positioned at $L \approx 0.2$ to obtain a 2 times enhancement of the feedback current, while disk electrodes reach the same feedback current at $L \approx 0.5$ (Figure 2a). The reason for the relatively smaller feedback at conical electrodes with conductive substrates can be explained as follows. Far from a substrate, the diffusion to the UME tip achieves a spherical diffusion layer, whose dimensions are predominately determined by the base radius a so that the behavior is rather disklike. However, when the electrode is very close to a conductive

substrate, the diffusion layer is disturbed by the substrate before reaching a spherical diffusion field and the dimensions of the diffusion layer are largely represented by the aspect ratio H of the conical surface and the feedback currents decrease as the aspect ratio H increases. That is, as H increases, less of the electrode surface is available to engage in feedback with the substrate, leading to a decrease in feedback currents. For example, I_T increases from a normalized bulk value of unity to 35.6 ($H = 0$), 11.1 ($H = 0.1$), 4.7 ($H = 0.3$), 3.2 ($H = 0.5$), 2.1 ($H = 1$), 1.6 ($H = 2$), and 1.4 ($H = 3$) at $L = 0.01$. Thus, for finite conical tips with $H > 1$, the feedback compared to $I_{T,\infty}$ is less than 2.

For insulating substrates, SECM feedback responses are also dependent on H, as shown in Figure 2b. For example, I_T decreases from a normalized bulk value of unity to 0.02 ($H = 0$), 0.17 ($H = 0.1$), 0.36 ($H = 0.3$), 0.48 ($H = 0.5$), 0.64 ($H = 1$), 0.76 ($H = 2$), and 0.80 ($H = 3$) at $L = 0.01$. When the SECM tip is positioned close to an insulating substrate, the substrate hinders the diffusion of species O from the bulk solution to the electrode surface so that the tip current decreases to a value lower than $i_{T,\infty}$ (negative feedback). However, as H increases in value, more of the electrode surface is accessible to the diffusing species O from bulk solution so that the negative feedback current becomes only marginally different from $I_{T,\infty}$ as can be seen for $H > 1$.

Overall then, for $H > 3$, little feedback is observed at a conical electrode because the contribution of reactant diffusing to the shaft of the electrode is much more important than that between the sharp end of the tip and the substrate. In general, even at smaller H values, the conical tip response is less sensitive to d than that of a disk.

Effect of Insulating Sheath Thickness on SECM Approach Curves. Many previous SECM studies assume a thick insulating sheath of approximately RG = 10.[21] In practice, however, the thickness is usually smaller, especially in the fabrication of the tips reported here and by others. To study the effect of RG on the SECM response for a finite conical electrode, theoretical SECM curves with different RG values and fixed H ratios were obtained. For example, Figures 3 and 4 show the effect of RG when $H = 0.5$ and 2.0, respectively. With insulating substrates (Figures 3b and 4b), a smaller RG value results in a higher current at any distance between the tip and substrate because the contribution of the mediator diffusion from behind the shield is not negligible when the thickness of the insulator shield is thin. Thus the magnitude of the negative feedback currents increase as RG decreases. This behavior occurs irrespective of the value of H and in this way is similar to that reported for disk[29,31] and ring electrodes.[26] As H increases, however, the change in the approach curves decreases significantly when $H > 1$, as shown in Figure 2b, and this carries over to the variation with RG. For example, comparison of Figure 3b where $H = 0.5$ with Figure 4b where $H = 2.0$ shows that the dependence on RG is much less for $H = 2.0$.

The SECM approach curve over a conductive substrate (Figures 3a and 4a) for any H does not vary as much with RG, because the diffusion of O from the bulk solution to the electrode surface makes a smaller contribution to the tip current as the tip approaches the substrate. Thus, as the insulating sheath becomes thinner, $i_{T,\infty}$ increases and the normalized feedback currents decrease. The result is that slightly less feedback enhancements are observed as RG values decrease as shown in Figures 3a and 4a. For $H > 1$, these feedback effects with RG are similar in magnitude to those found over an insulator.

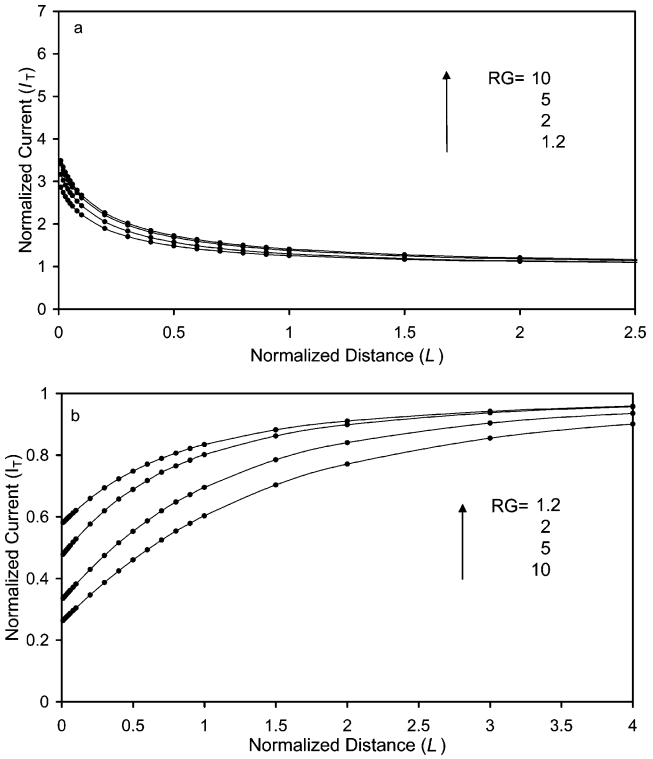

Figure 3. Theoretical SECM feedback responses of finite conical microelectrodes at (a) conductive and (b) insulating substrates with various RG values while $H = 0.5$.

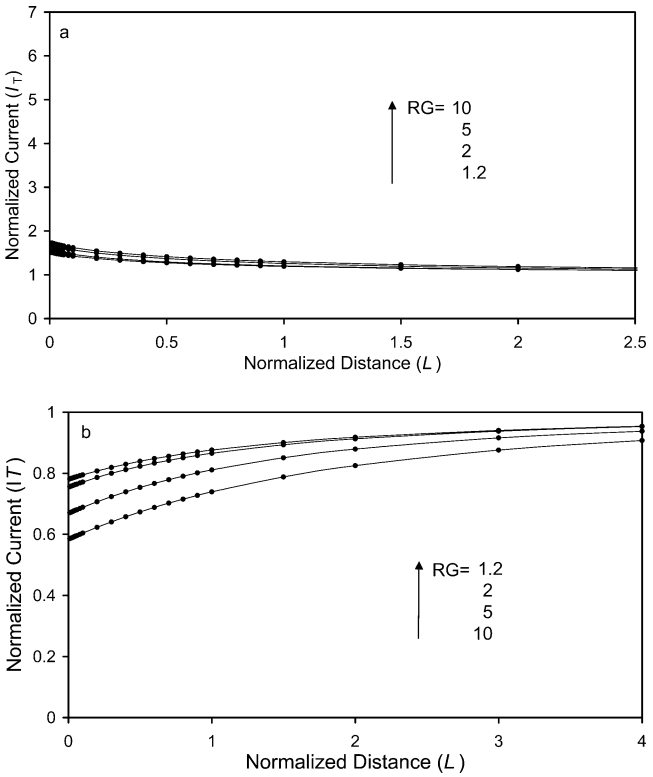

Figure 4. Theoretical SECM feedback responses of finite conical microelectrodes at (a) conductive and (b) insulating substrates with various RG values while $H = 2.0$.

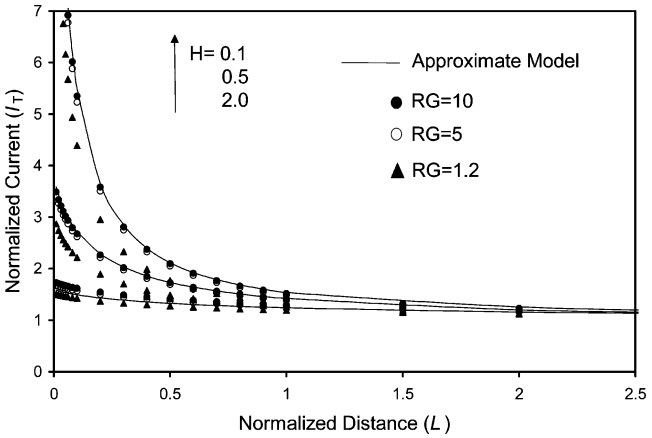

Figure 5. Comparison between positive feedback SECM curves based on the approximate model (solid lines) using eq 1 and the simulations in this work (symbols).

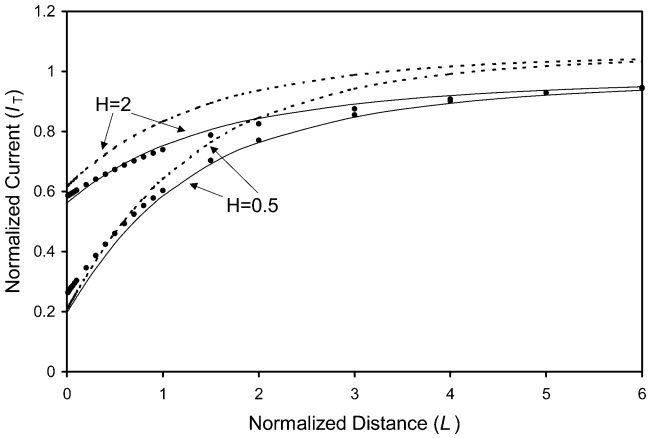

Figure 6. Comparison between negative feedback SECM curves based on the approximate model (dotted lines) using eq 2, the approximate model with revised feedback equations (solid lines), and the simulations in this work (solid dots). RG = 10.

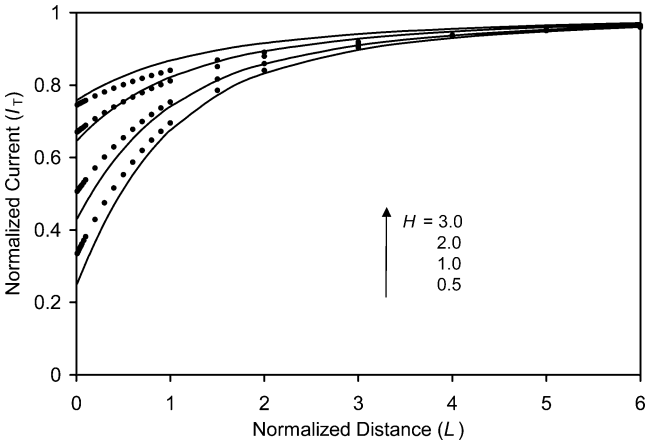

Figure 7. Comparison between negative feedback SECM curves based on the approximate model (solid lines) with revised feedback equations and the simulations in this work (solid dots). RG = 5.

In principle, information about the aspect ratio H of conical electrodes can be best extracted by analyzing SECM curves at conductive substrates where $H < 1$, because they only weakly depend on RG values. RG values can then be obtained by analyzing SECM curves at insulating substrates, where there is a strong dependency on the thickness of the insulating sheath. This is the approach that is standard practice in characterizing planar disk-shaped[21,29,31,38] and planar ring-shaped[26] tips. For $H > 1$, information about H and RG can be obtained using either an approach over an insulator or a conductor since the change in the magnitude of the approach curves with RG and H are similar in both cases. This is the strategy that was used in the experiments reported here.

Comparison to Earlier Model. Figure 5 shows a comparison of the simulated data for the approach of a finite conical UME tip to a conductive substrate with the approximate model[19] based on eq 1 for a range of H and RG values. The solid lines represent the approximate model approach curves for the specific H values while the symbols represent the results from the simulations in this work. There is good agreement between the simulated and approximated approach curves for RG values of 5 and 10. A larger deviation between simulated and approximated results is seen for RG = 1.2 as would be expected because there is a slight dependence of RG on approach curves over conductive substrates, as explained earlier.

Figure 6 shows a comparison of the simulated data (solid dots) with the approximate model based on eq 2 (dotted line) for the approach of a finite conical UME tip with an RG of 10 and H = 0.5, 2 to an insulating substrate. The normalized current from the approximate model becomes much larger than the simulated current as the UME tip is withdrawn from the substrate surface. The reason for this discrepancy can be explained as follows. As the insulating layer around a planar disk UME tip becomes thinner and RG decreases in value, there is enhanced diffusion from behind the plane of the UME tip so that $i_{T,\infty}$ is actually larger than the $i_{T,\infty}$ defined by eq 3 for an infinite RG. For an inlaid disk UME, this means that the factor of 4 in eq 3 becomes larger as RG becomes smaller. For example, factors of 4.06 (RG = 10), 4.43 (RG = 2), 4.64 (RG = 1.5), and 5.14 (RG = 1.1) have been reported.[11] Experimentally in SECM, steady-state currents recorded at an inlaid disk UME tip, for example, as it approaches a substrate are normalized by the $i_{T,\infty}$ measured far from the substrate surface. Essentially one is then normalizing by an $i_{T,\infty}$ for the specific RG of the UME tip. However, the approximate eqs 1 and 2[19] are based on the first simulated data[29] reported for SECM for disk UME tips. In these simulations, the effect of RG size was considered, but diffusion from behind the plane of the UME tip was not (although the authors noted that rigorous consideration of this effect would be required for more accurate simulations). Thus, enhanced simulated currents were seen as RG decreased in value from 1000 to 100 to 10 but all simulated currents were normalized by eq 3. This results in normalized currents that are larger in magnitude the further the UME tip is from the substrate as seen in Figure 6. However, if later approximate expressions for inlaid disk UME tips over insulating substrates, which take into account the back diffusion,[21,30,31] are used in place of eq 2, the solid lines in Figure 6 result showing much better agreement between simulated and approximated results. Figure 7 shows qualitative agreement between a family of approximate curves (solid line) and simulations (solid dots) from this work for RG = 5, where reported inlaid disk expressions for approach curves at this RG value were used.[31]

(38) Zoski, C. G. *Electroanalysis* **2002**, *14*, 1.

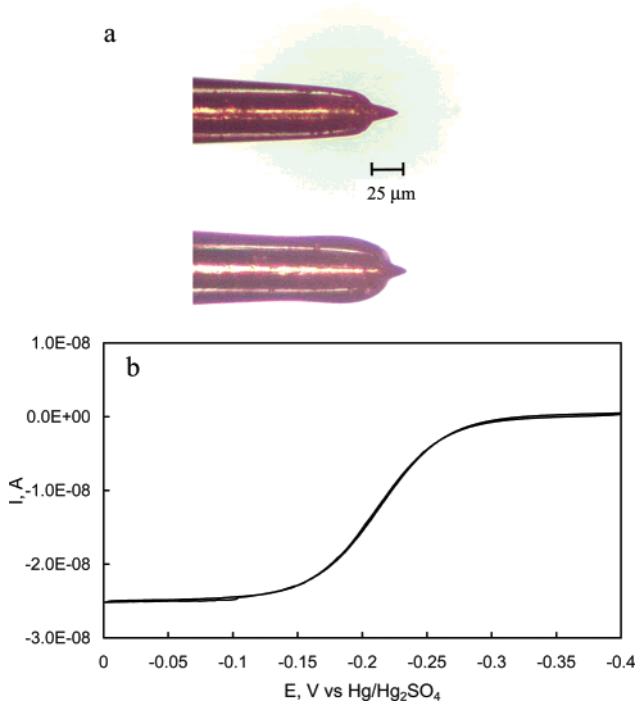

Figure 8. Optical images of two conical Pt tips (a) and the corresponding steady-state voltammogram. Solution is 1 mM ferrocenemethanol in 0.1 M KCl.

Table 2. Tabulation of Optical Measurements and Fitting Results of Five Different Glass-Sealed, Finite Conical Tips

	optical measurements		fitting results			
tip	$h \pm 2\ \mu$m	$a \pm 2\ \mu$m	a (μm)	h (μm)	H	RG
1	22	8	7	14	2	1.2
2	13	5	7	14	2	1.2
3	23	8	7	14	2	2
4	15	5	8	16	2	2
5	15	5	6	12	2	2

Thus, there is reasonable agreement between the simulations of this work and the approximate model based on eq 1 when the approach is over a conductor since these approach curves are less sensitive to the RG of the UME tip. However, when the approach is over an insulator, the equation used in the approximate model becomes important, and analytical expressions (which are reported in the literature) for specific RG values[21,30,31] must be used in place of eq 2.

Determination of the Base Radius, Aspect Ratio, and Thickness of the Insulating Sheath. Figure 8 shows the optical images for two representative conical Pt tips and the steady-state voltammogram for one of these finite conical UME tips in an aqueous solution of 1 mM ferrocenemethanol. A sigmoidal steady-state voltammogram with little hysteresis between the forward and reverse potential sweeps, as shown, is an indication of a good seal between the glass insulation and the Pt in the fabrication of these finite conical UMEs. Table 2 lists the height and base radius parameters that were estimated from optical micrographs for five finite conical Pt tips. The optical images in Figure 8a correspond to tip 1 (top image) and tip 2 (bottom image) in Table 2. In making these measurements, it was often difficult to find the exact point at which the glass insulation began. Thus, an error of two divisions on the microscope micrometer (1 μm/division) was assigned to the optical measurements of h and a tabulated in Table 2.

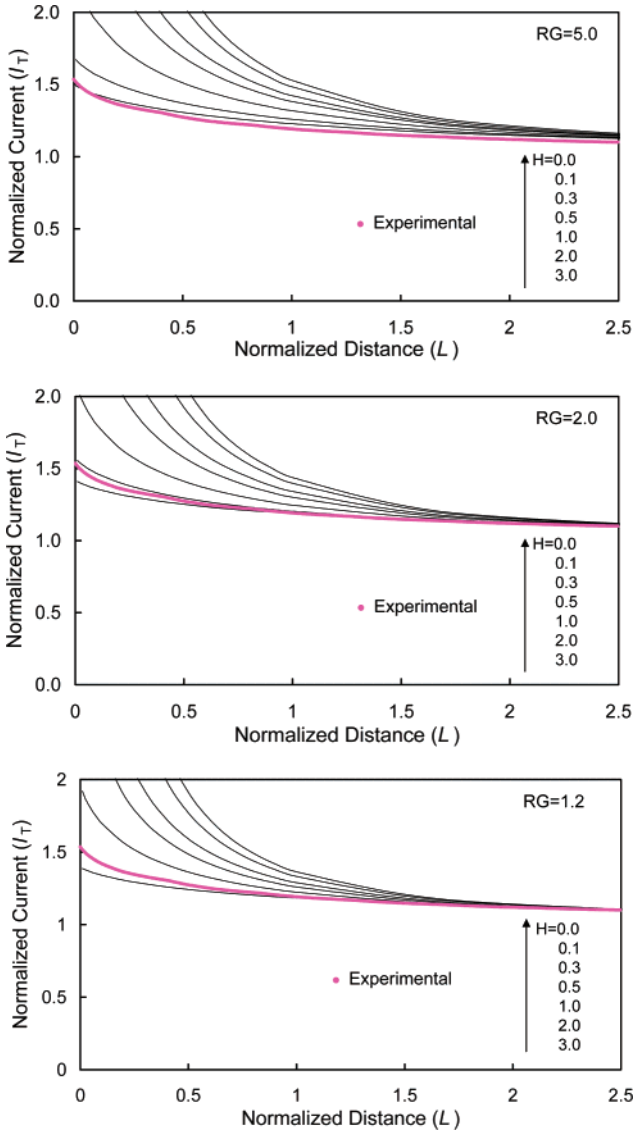

Figure 9. Comparison of the theoretical (solid lines) and experimental SECM (dotted line) curves at a Pt conductive substrate at the indicated H and RG values. A 1 mM ferrocenemethanol aqueous solution was used with 0.1 M KCl as the supporting electrolyte. The tip and substrate were held at potentials of −0.05 and −0.4 V, respectively, vs Hg/Hg_2SO_4. The best fit was obtained for $H = 2$ and RG = 1.2.

Figure 9 shows the fitting of an experimental approach curve as the tip approaches a conductor (positive feedback). The small positive feedback under diffusion-controlled feedback conditions is an indication that the tip has an aspect ratio greater than the zero characteristic of an inlaid disk. In fitting the positive feedback approach curve data, a family of curves for aspect ratios of $H =$ 0.1, 0.3, 0.5, 1.0, 2.0, and 3.0 at RG values of 10, 5, 2, and 1.2 were constructed. The experimental approach curve data was overlaid on each of these graphs, three of which are shown in Figure 9 for tip 2 in Table 2. The best fit of the positive feedback approach curve data for this finite conical tip with the simulated data is found for $H = 2$ and RG = 1.2. A base radius of 7.0 μm was used in the

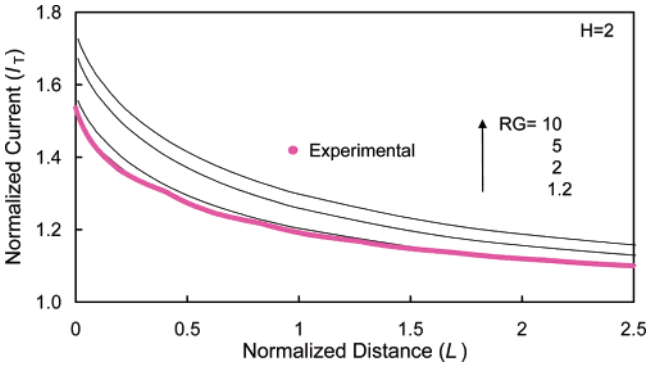

Figure 10. Comparison of the theoretical (solid lines) and experimental SECM (dotted line) curves at a Pt conductive substrate at $H = 2$ for RG values of 10, 5, 2, and 1.2. Theoretical curves (solid lines) and normalized experimental curves (dotted line) were obtained over a Pt conductive substrate in an aqueous solution containing 1 mM ferrocenemethanol/0.1 M KCl. The tip and substrate were held at potentials of −0.05 and −0.4 V, respectively, vs Hg/Hg_2SO_4. The best fit was obtained with an RG of 1.2.

fitting, corresponding to an h of 14 μm, in good agreement with the optical measurements reported for tip 2 in Table 2. Thus, tip 2 can be described by $H = 2$, $a = 7.0$ μm, and RG = 1.2. This fit can be more clearly seen in Figure 10, which shows a plot of the normalized current for $H = 2$ as a function of RG. The fitting results from the approach curve over a Pt substrate for tip 1 in Table 2 were obtained similarly. Because the approach curves are not very sensitive to H in the region of $3 < H < 2$, there is more uncertainty in this value than there would be for smaller values of H.

Tips 3−5 were characterized using an approach over an insulator (negative feedback). As can be seen from evaluation of Table 2, the fitting results are in reasonable agreement with the optical measurements, given the sizable uncertainties in both techniques. Figures 11 and 12 show the fitting of the approach curve data with the simulated data corresponding to tip 5 in Table 2. Thus, this tip can be characterized by the geometric parameters including $H = 2$, $a = 6$ μm, and RG = 2. Note that all of these measurements were made with virgin tips that never experienced a crash with the surface. Even slightly touching the substrate surface (a "soft crash") significantly changed the conical disk parameters, so that it was not possible to obtain both conductive and insulating approach curves with the same tip.

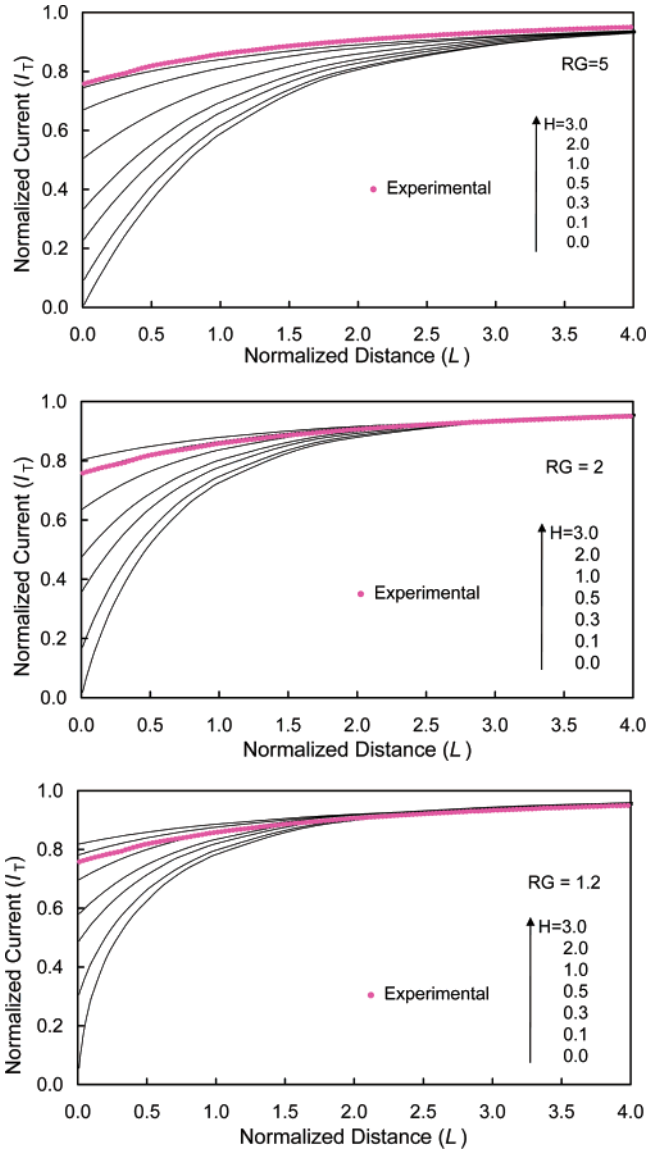

Figure 11. Comparison of the experimental SECM curve (dotted line) to theoretical ones (solid line) over an insulating substrate for different values of H and RG. The normalized experimental curve was obtained over the insulating part of a Pt substrate in an aqueous solution of 1 mM ferrocenemethanol/0.1 M KCl. The tip and substrate were held at potentials of −0.05 and −0.4 V respectively, vs Hg/Hg_2SO_4. The best fit was obtained with $H = 2$ and RG = 2.

CONCLUSIONS

SECM tip current−distance (approach) curves for finite conical UMEs were calculated using finite element analysis. The normalized diffusion-limited steady-state currents of finite conical UMEs were calculated at various relative distances (L) between the UME tip and either a conducting or insulating substrate. The theoretical SECM curves at conductive and insulating substrates are both influenced by the aspect ratio H, although the influence is more significant over a conductor for $H \leq 1$ where I_T values greater than 2 are possible. The positive feedback effect with finite conical UMEs is less than that of a disk UME; that is, as the conical UME becomes sharper, the extent of positive feedback decreases and reaches a finite value. In contrast, SECM curves at insulating substrates depend dramatically on RG for $H \leq 1$. For $H > 1$, the effect of RG is similar on approach curves over conductors or insulators.

The simulated data were compared to data generated using an approximate model based on analytical expressions that had been derived for approach curves between a disk UME and substrate. The approximate model was found to be in reasonable agreement with the simulated data reported here as long as analytical expressions that take into account diffusion from behind the insulating sheath of the disk UME are used.

Experimental approach curve data were compared to simulated data. In fitting the experimental data, graphs of normalized current I_T versus normalized distance L were created for H values ranging from 0 to 3 at constant RG values of 10, 5, 2, and 1.2. From these graphs, the geometrical parameters $H = 2$, $a = 7 \pm 1$ μm, $h = 14 \pm 2$ μm, and RG between 1.2 and 2 were determined for five etched electrodes. These values were in good agreement with those measured using an optical microscope.

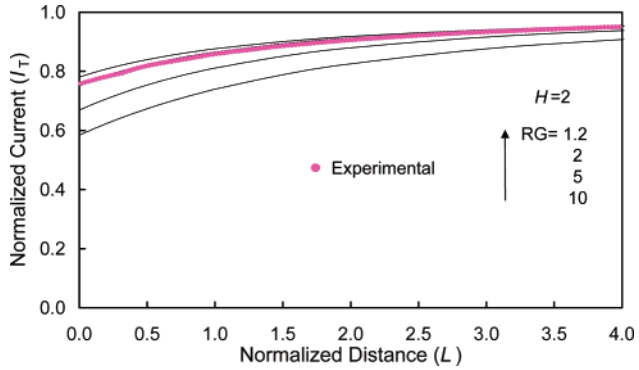

Figure 12. Comparison of the theoretical (solid lines) and experimental SECM (dotted line) curves at a Pt conductive substrate at $H = 2$ for RG values of 10, 5, 2, and 1.2. Theoretical curves (solid lines) and normalized experimental curves (dotted line) were obtained over an insulator in an aqueous solution containing 1 mM ferrocenemethanol/0.1 M KCl. The tip and substrate were held at potentials of −0.05 and −0.4 V respectively, vs Hg/Hg_2SO_4. The best fit was obtained with an RG = 2.

The good fits that are possible between experimental data for the etched UMEs with the simulation data for a finite conical geometry provide confidence that the assignment of a conical geometry to these etched electrodes is appropriate. Moreover, the sensitivity of SECM to the shape parameters including H, h, a, and RG provides a definitive method of characterizing etched electrodes that is not possible using steady-state limiting currents. However, to use SECM in characterizing these etched electrodes, the approach to the substrate must be carefully controlled so that the etched electrode does not touch the substrate surface. Thus, a disadvantage of conical tips is the inability to restore the tip to near its original dimensions by polishing following a "tip crash", as is frequently done with disk-shaped tips. Thus conical tips will continue to find the greatest application in SECM in substrate generation/tip collection experiments[21] rather in than in feedback ones where the tip must be close to a substrate surface. A complimentary investigation of conical-shaped electrodes with SECM has recently been brought to our attention.[39]

(39) Xiong, H.; Guo, J.; Kurihara, K.; Amemiya, S. *Electrochem. Commun.*, in press.

ACKNOWLEDGMENT

This work has been supported by grants from the National Science Foundation (CHE-0210315 to C.G.Z. and CHE-0109587 to A.J.B.).

SUPPORTING INFORMATION AVAILABLE

Two simulation programs for SECM over an insulator and conductor with a conical UME. This material is available free of charge via the Internet at http://pubs.acs.org.

Received for review January 10, 2004. Accepted March 31, 2004.

AC049938R